JOURNAL OF Applied Polymer SCIENCE

Experimental Characterization of a Curing Thermoset Epoxy-Anhydride System—Isothermal and Nonisothermal Cure Kinetics

Xiaosong Huang,[1] Bhaskar Patham[2]
[1]Chemical Sciences & Materials Systems Lab, GM Global R&D, Warren, Michigan
[2]India Science Lab, GM Global R&D, Bangalore, Karnataka, India
Correspondence to: X. Huang (E-mail: xiaosong.huang@gm.com)

ABSTRACT: This work describes in detail the kinetic model for the cure of an epoxy-anhydride thermoset matrix resin system. The cure kinetics in both nonisothermal and isothermal modes has been characterized using differential scanning calorimetry. The Sestak–Berggren two-parameter autocatalytic model was used to describe the nonisothermal cure behavior of the resin satisfactorily. The isothermal cure data was fitted with Kamal's four-parameter autocatalytic model, coupled with a diffusion factor. These characterization data will form material property inputs for a multiscale modeling framework for the estimation of cure-induced residual stresses in thick thermoset matrix composites. © 2012 Wiley Periodicals, Inc. J. Appl. Polym. Sci. 000: 000–000, 2012

KEYWORDS: cure kinetics; thermoset; epoxy; nonisothermal; isothermal; residual stress

Received 5 January 2012; accepted 23 February 2012; published online
DOI: 10.1002/app.37567

INTRODUCTION

During the cure of any thermoset resin system—unfilled, filled, impact-modified, or fiber-reinforced—the mechanical properties (such as modulus, strength, and fatigue behavior) build progressively with the increase of the degree of cure, as the resin (or matrix) starting from a viscous state, crosslinks into a rubbery gel, and ultimately into an elastic solid. The mechanical properties of the cured part are significantly impacted by the final degree of cure attained, the uniformity of cure, and the residual stresses associated with thermal and crosslink-shrinkage strains in combination with imposed mechanical constraints during the cure.[1] To ensure complete and uniform cure, an informed decision regarding the choice of cure cycle (e.g., Ref. 2) can only be made with a detailed process model that accurately takes into account (1) the geometry of the part, (2) the thickness of the section, (3) the kinetics of cure, (4) the exothermic heat associated with the cure reaction, (5) the properties of the resin governing heat transfer such as density, thermal conductivity, and specific heat, and (6) the thermal boundary conditions. Additionally, any decisions regarding strategies to mitigate the detrimental effects of process-induced residual stresses—including process modification, or mold shape compensation (cf. Ref. [3])—need to be guided by residual stress simulations that in addition to (1–6) above, take into account (7) the temperature-, degree-of-cure-, and time-dependence of the resin modulus, (8) the temperature- and degree-of-cure-dependent coefficient of thermal expansion, (9) the evolution of shrinkage strains with the degree of cure, (10) the gel point of the curing resin, (11) the cure-dependent glass transition temperature of the thermoset, (12) the mechanical boundary conditions, and (13) any additional microstructural features of relevance to the development of residual stresses, such as voids, resin rich areas, and fiber rich regions.

The overall objective of this research is to develop a multiscale modeling framework to arrive at more realistic estimates of residual stresses in the vicinity of the fiber-matrix interface in thick thermoset composites. The accuracy and relevance of this modeling framework will be most significantly governed by the detail and precision with that the properties of the individual components of the composite are accounted. The thermo-mechanical properties of the reinforcing fiber typically do not change drastically during the course of a cure cycle (e.g., Refs. 4,5); however, the kinetics of cure and the thermo-rheological properties of the matrix resin are strongly influenced by the transients of the degree of cure and the temperature cycle. Despite the significant impact of these parameters on the residual stress development, comprehensive experimental studies on the property estimation of curing thermoset resin systems addressing the kinetics, rheology, and chemo-thermo-mechanical properties of the resin system are not widely reported (Refs. 6, 7 are two examples of comprehensive characterization studies of curing thermoset resins). The lack of detailed experimental

characterization information often results in the need for simplistic assumptions for material properties in simulations, thus adversely impacting their accuracy.

This work describes in detail the experimental study of the evolution of degree of cure transients of a thermoset resin system using differential scanning calorimetry (DSC), and the kinetics models that best describe these transients in dynamic (temperature ramp,) and isothermal scenarios. The rheological and thermo-mechanical characterization of the resin and the associated material models for cure-, and temperature-dependent evolution of the thermo-chemo-mechanical properties of the resin will be described in the future.

EXPERIMENTAL

Materials

A thermoset epoxy-anhydride resin system from Huntsman was chosen for the characterization studies. This resin system, which is commercially available for filament winding, consists of three components: (1) the resin Araldite LY556 is a diglycidyl ether of bisphenol A type epoxy resin; (2) the hardener Aradur HY917 is methyl tetrahydrophthalic anhydride; and (3) the accelerator DY070 (LY556) is 1-methyl-imidazole. The choice of the Huntsman system was guided by an earlier screening study of matrix resin systems for application in high pressure hydrogen storage vessels, in which this system was found to satisfy the following major benchmarking requirements:

- Glass transition temperature of the fully cured matrix resin must be greater than the operating temperature of the composite part;
- Strain to failure of the fully cured matrix resin is recommended to be twice that of the fiber (carbon fibers);
- Cure temperature of the matrix resin must be lower than the polymeric (HDPE) liner's melt temperature ($\sim$ 120°C);
- Viscosity at room temperature (RT) of the uncured matrix resin system should be low for effective wetting of fibers.

For the cure-kinetics and property-evolution characterization experiments, the resin, hardener, and accelerator were mixed at room temperature in 100 : 90 : 1 ratio by weight.

Differential Scanning Calorimetry Experiments

Reaction kinetics was investigated through temperature modulated DSC. A Q-2000 DSC from TA Instruments was used for both isothermal and nonisothermal experiments. Prior to the experiment, the resin-hardener-accelerator compound was thoroughly mixed, and degassed.

For nonisothermal kinetics, the samples were sealed in a hermetic pan and scanned from room temperature to 250°C at constant rates of 2, 5, 10, and 20°C/min. The total heat of reaction, H_T, was estimated by integrating the area under the exothermic peak. The average H_T, measured from the nonisothermal DSC experiments at the four constant heating rates was 327.2 $\pm$ 9.6 J/g.

Isothermal cure was conducted at 100, 110, 120, 130, 140, and 150°C for 120 min. The epoxy samples were sealed in a hermetic pan and rapidly heated to the cure temperature. All the isothermal curves leveled off to the baseline at the end of the scan. To determine the conversion at any given time t, the area under the exotherm curve up to time t was divided by the total heat of reaction for the complete cure. To determine any residual heat of reaction, samples were cooled to room temperature rapidly after the completion of each isothermal scan and reheated to 250°C at 10°C/min. The residual heat for each isothermal cure was then estimated by integrating the reheating curves.

THEORETICAL BACKGROUND, RESULTS, AND DISCUSSION

Several phenomenological and mechanistic models have been proposed to describe thermoset cure kinetics.[8–19] Epoxy cure is a complicated process and the reaction mechanism is still subject of considerable research. Phenomenological models are popular for epoxy resin systems due to their simplicity. In a phenomenological model, the degree of conversion (α) can be calculated using the following formula, given the assumption that there is a single predominant reaction and that there are no other enthalpic events in the cure process.

$$\alpha = 1 - \frac{H_r}{H_T} \tag{1}$$

where H_r and H_T are the residual heat of reaction (at conversion α) and the total heat of reaction, respectively.

Nonisothermal Cure Kinetics

The analysis of nonisothermal or dynamic kinetics is quite complicated, since the sample during dynamic cure may progress through multiple reactions, each of which may have a different temperature dependence. A simplifying assumption involves the description of the reaction rate $\frac{d\alpha}{dt}$ as a product of two functions, one of which is solely a function of temperature, $k(T)$, and the other that is solely a function of conversion, $f(\alpha)$, as shown below:[8–11]

$$\frac{d\alpha}{dt} = k\,(T) \cdot f(\alpha) \tag{2}$$

An Arrhenius relationship is typically used for the temperature dependent function. Thus,

$$\frac{d\alpha}{dt} = Ae^{\left(-\frac{E_a}{RT}\right)} \cdot f(\alpha) \tag{3}$$

where A is the preexponential factor, E_a is the apparent activation energy, R is the ideal gas constant, and T is the absolute temperature in Kelvin. Now the analysis of kinetics involves the estimation of$A$, E_a, $f(\alpha)$. To estimate the activation energy, E_a, an isoconversion method is used—which involves the determination of the temperature corresponding to a fixed degree of conversion in dynamic DSC experiments carried out at several heating rates. The Kissinger method,[20] which is a special case of the Kissinger–Akahira–Sunose (KAS) model[20,21] is a simple method to calculate E_a; it is based on the assumption that the conversion corresponding to the maximum rate of reaction during dynamic cure remains a constant (independent of heating rates), and therefore involves the measurement of the temperature (T_p)

corresponding to the maximum reaction rate at various heating rates (β).[20,21] The integral form of the Kissinger equation is shown below.[20,21]

$$-\ln\left(\frac{\beta}{T_p^2}\right) = \frac{E_a}{RT_p} - \ln\left(\frac{AR}{E_a}\right) \quad (4)$$

E_a can then be calculated from the slope of the plot of $-\ln\left(\frac{\beta}{T_p^2}\right)$ against $\frac{1}{T_p}$. The E_a for the epoxy-anhydride cure reaction obtained from this method is 76.37 kJ/mol. This isoconversion method can only provide a single E_a for the whole reaction process. The real cure process may include many complicated chemical reactions with different activation energies. Therefore, the calculated E_a is an apparent activation energy that represents all the reactions in the epoxy cure. A single E_a can simplify the mathematical calculation and is generally sufficient to generate a valid phenomenological model.

The next step involves the estimation of the kinetic factor $f(\alpha)$. The applicability of Sestak–Berggren equation (a two parameter autocatalytic model), which has been used to model the cure of both amine-cured and anhydride-cured systems in several studies[8–11,22] was tested to analyze the nonisothermal kinetic data. In the two parameter Sestak–Berggren autocatalytic model, $f(\alpha)$ is expressed as shown in eq. (5).

$$f(\alpha) = \alpha^m(1-\alpha)^n \quad (5)$$

where m and n are kinetic exponents. Equation (5) is the Sestak–Berggren equation assuming that termination reactions are negligeable, which has shown to work well in the autocatalytic curing reactions[8–11,22]. Sestak–Berggren equation is normally expressed as $f(\alpha) = \alpha^m(1-\alpha)^n\ (-\mathrm{lm}(1-\alpha))^p$,[11] where m, n, and p are all kinetic exponents. Substituting $f(\alpha)$ in eq. (5) into eq. (3), and taking the logarithm of both sides results in the form shown in eq. (6).

$$\ln\left(\frac{d\alpha}{dt}e^{\frac{E_a}{RT}}\right) = n\cdot\ln[\alpha^p(1-\alpha)] + \ln A \quad (6)$$

where $p = \frac{m}{n}$. p may be evaluated using the following relationship:

$$p = \frac{\alpha_M}{1-\alpha_M} \quad (7)$$

α_M is the peak maxima determined from the $\left(\frac{d\alpha}{dt}\right)e^{\frac{E_a}{RT}}$ versus α curves at different heating rates. n can then be obtained from the plot of $\ln\left(\frac{d\alpha}{dt}e^{\frac{E_a}{RT}}\right)$ against $\ln[\alpha(1-\alpha)^p]$, and m can be calculated using eq. (7), substituting the values of n and p.

Figure 1 shows the evolution of conversion with increase in temperature at different heating rates. The conversion evolves in a sigmoidal fashion with temperature, increasing slowly at the initial stage, followed by a regime of rapid increase, and leveling off at the final stage. This indicates that the cure reaction takes place rapidly in a narrow temperature range. The sigmoidal portions of the curves shift successively right (higher temperatures) with increasing heating rate. The curves of $d\alpha/dt$ (rate of reaction) versus temperature at different heating rates are plotted in Figure 2. As observed in Figure 1, the rate of reaction is very low in both the early and the late stages of the dynamic temperature ramp. A maximum reaction rate can be observed in the range from 100 to 200°C depending on the heating rates. With increase in heating rate, the temperature corresponding to the maximum reaction rate increases.

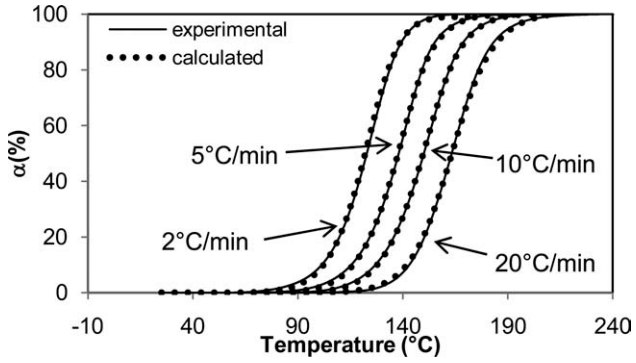

Figure 1. Evolution of degree of cure with temperature during nonisothermal cure at different heating rates (Solid curves indicate the experimental data and dotted curves indicate the fits obtained with the two-parameter Sestak–Berggren model using parameters listed in Table I).

In Table I, the cure activation energy evaluated using the Kissinger isoconversion technique, and the kinetic model parameters for Sestak–Berggren equation used for fitting the nonisothermal cure transients are listed for the epoxy-anhydride system. The total reaction order ($m + n$) was found to be 1.69. The kinetic model fits using the parameters in Table I for conversion and rate of reaction are also displayed in Figures 1 and 2, respectively (as dotted lines). A good fit can be observed from Figures 1 and 2 for all four heating rates. It may be concluded that the Sestak–Berggren two parameter autocatalytic model accurately describes the dynamic cure processes at the four heating rates studied.

Isothermal Cure Kinetics

The nth-order and autocatalytic kinetics are the two most commonly used reaction mechanisms that describe isothermal cure.[12–15] The nth-order kinetic model can be expressed as shown in eq. (8)[12,13]

$$\frac{d\alpha}{dt} = k(T)(1-\alpha)^n \quad (8)$$

where n is the reaction order and $k(T)$ is a temperature dependant rate coefficient.

The Kamal equation was originally developed to describe the stepwise reaction mechanism of amine cured epoxy resin and can be expressed as shown in eq. (9)[14,15]

$$\frac{d\alpha}{dt} = (k_1 + k_2\alpha^m)(1-\alpha)^n \quad (9)$$

k_1 and k_2 are the temperature dependent reaction rate coefficients for noncatalytic and autocatalytic reactions, and m and n are reaction orders. k_1 and k_2 follow the Arrhenius relationship and can be described as below:

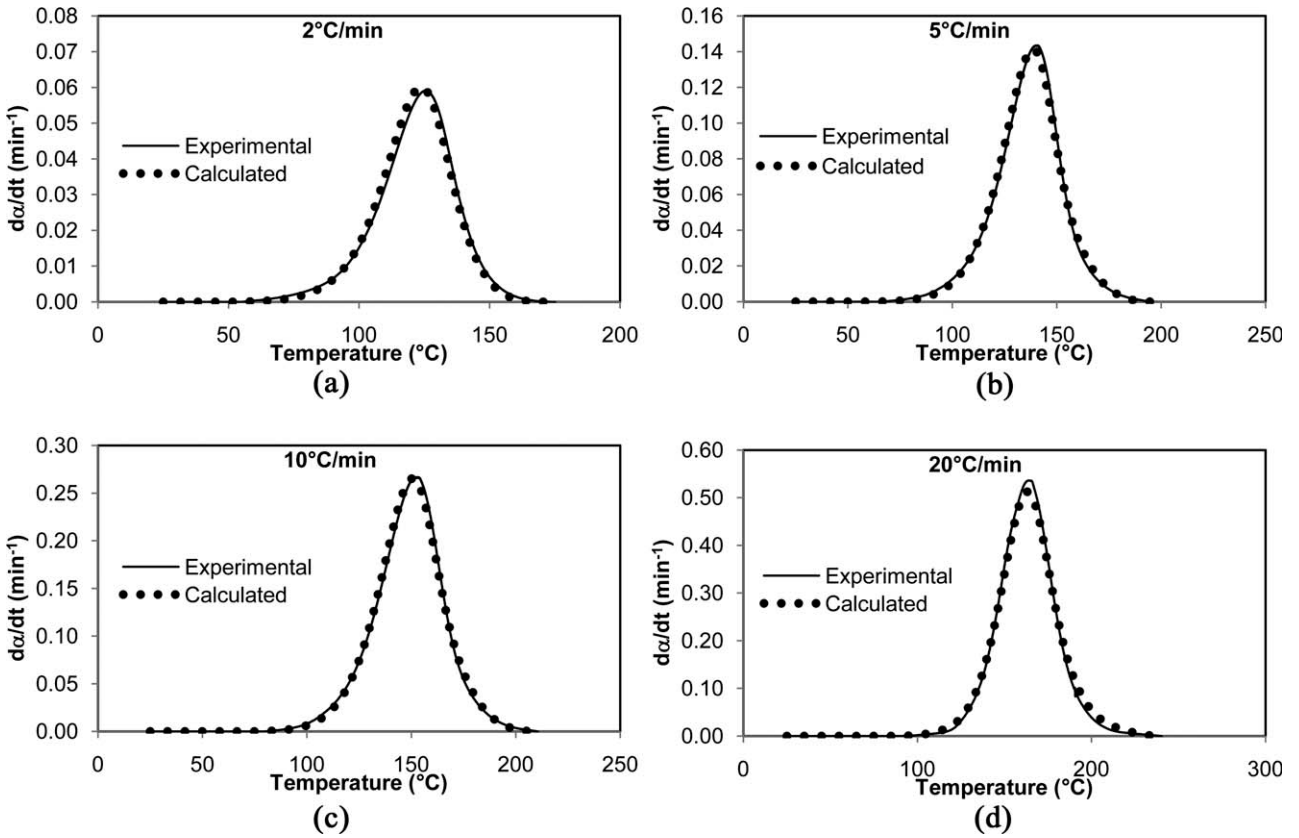

Figure 2. Evolution of the rate of the cure reaction with temperature during the nonisothermal cure at different heating rates (indicated in each panel). The calculated fits are obtained with the two-parameter Sestak–Berggren model using the parameters listed in Table I.

$$k_1 = A_1 e^{\left(-\frac{E_{a1}}{RT}\right)} \tag{10}$$

$$k_2 = A_2 e^{\left(-\frac{E_{a2}}{RT}\right)} \tag{11}$$

A_1 and A_2 are the preexponential factors, and E_{a1} and $E_{a2}$are the apparent activation energies for k_1 andk_2, respectively.

The experimentally calculated transient of the reaction rate, $d\alpha/dt$ for isothermal cure is plotted in Figure 3 at different isothermal cure temperatures ranging from 100 to 150°C. At the very beginning of the isothermal cure, there is a short period of time that is required for temperature stabilization. The data in this period is not very reliable. It can be clearly seen in Figure 3 that the maximum rate of conversion is achieved in the middle of the reaction, rather than at the beginning; this is characteristic of autocatalytic reactions. Subsequently, the reaction rate decreases, and the remaining cure occurs at a relatively low rate of reaction, resulting in a long tail in the plot. The reactions progress fast in the early stages of cure because of the low resin viscosity and the large amount of reactive groups available for the cure reaction. It has been reported that the production of intermediate groups can catalyze the cure reaction; therefore an autocatalytic model is generally known to fit the experimental data well in these early stages.[14–16,22] In the later stages of cure, with the mobility of the reactive species hindered by the increased viscosity of the crosslinking resin, the rate of reaction is controlled by diffusion rather than by reaction kinetics. Therefore, the reaction proceeds at a much slower rate and takes a relatively long time to reach completion. Figure 4 shows the curves of conversion versus time. Consistent with the variation of reaction rates with the degree of cure shown in Figure 3, the conversion increases rapidly in the early stages of cure, and levels off at the later stages. It should also be noted from Figure 4, that at the lower cure temperatures, the curves level off at a lower degree of cure as compared to those at higher temperatures. These trends are indicative of strong diffusion effects.

The presence of diffusion effects are more clearly discernible in plots of experimentally determined reaction rate versus conversion, shown in Figure 5 at different isothermal cure temperatures. It is clear from these plots that the reaction rate peaks at an intermediate conversion (rather than at zero conversion), consistent with the autocatalytic nature of the reaction (however, the autocatalytic peaks should be differentiated from the sharp, small peaks that occur at the very beginning of the experimental curves, which appear to be caused because of the

Table I. Calculated Parameters for the Nonisothermal Kinetic (KAS) Model

lnA [ln(min^{-1})]	E_a (kJ/mol)	m	n
21.55	76.37	0.39	1.30

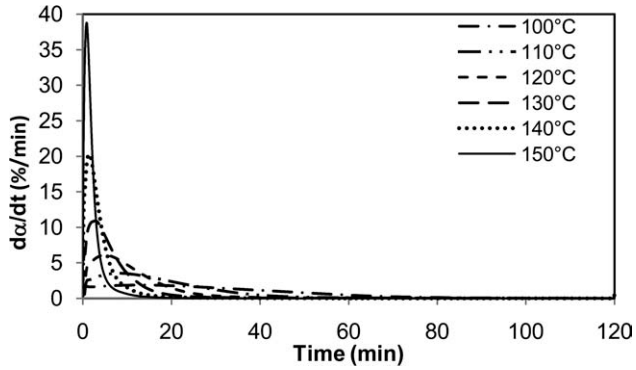

Figure 3. The transients of the rate of the cure reaction at different isothermal cure temperatures.

equilibration of temperature, and therefore can be treated as experimental errors). More significantly, the reaction rates clearly reduce to zero at ultimate conversions, α_c, which are different from 100%, indicating that diffusion effects may be preventing the reaction from completing. Also, the ultimate conversion corresponding to zero reaction-rate clearly decreases with decrease in cure temperature. It is therefore clear that the isothermal kinetic model needs to account for diffusion effects.

Several mathematical treatments have been investigated to include diffusion effects.[14–16,22–26] Fournier et al.[23] proposed an equation for diffusion factor based on Cole's equation shown below in eq. (12).[24]

$$f(\alpha) = \frac{k_e}{k_c} = \frac{2}{1 + e^{(\alpha - \alpha_c)/C}} - 1 \qquad (12)$$

where k_c is the rate coefficient for the chemical kinetics and k_e is the overall effective rate coefficient. In this equation, α_C is the final conversion at the given cure temperature, and C is an empirical constant. In the early stages of cure, the reaction is chemically controlled and $f(\alpha)$ is very close to unity. As α approachesα_C, the reaction becomes increasingly diffusion controlled, and $f(\alpha)$ becomes zero at α_C. The modified Kamal's model, after incorporation of the diffusion factor defined in eq. (12), can then be expressed as:

$$\frac{d\alpha}{dt} = (k_1 + k_2\alpha^m)(1-\alpha)^n\left(\frac{2}{1 + e^{(\alpha - \alpha_C)/C}} - 1\right) \qquad (13)$$

Thus, in the early stages of reaction, this model is similar to autocatalytic reaction kinetic model, while at higher degrees of cure it tends to become increasingly diffusion limited; at the ultimate conversion, α_C, at any given temperature of cure, this model predicts a zero reaction rate.

The fits to experimental reaction rate versus conversion data, obtained with the purely autocatalytic Kamal model [eq. (9)], and the modified Kamal model with the diffusion factor incorporated [eq. (13)], are also displayed in Figure 5. The associated model parameters for the two models are listed in Table II. The model parameters, k_1, k_2, m, and n, associated with the Kamal autocatalytic model at any given isothermal cure temperature were generated using experimental reaction rate data up to a conversion of 65% (the entire degree of cure transient was not considered because of the predominance of diffusion effects at later stages). k_1 and k_2 increase with increase in cure temperature. Using eqs. (10) and (11), E_{a1} and E_{a2} were calculated to be 59.52 and 89.78 kJ/mol, respectively. Different reaction orders (m and n) were obtained at different temperatures, which indicate that the cure may involve complicated reactions. The kinetic parameters obtained from this fitting exercise are apparent ones and cannot be used to explain the underlying reaction mechanisms. The different reaction orders associated with different cure temperatures also indicate that the cure kinetics is heavily dependent on thermal history. Therefore, the parameters obtained at one temperature cannot be directly used for another temperature without interpolation/extrapolation. With these temperature-dependent k_1, k_2, m, and n, listed in Table II, the parameter C in the diffusion factor was then calculated using eq. (13). As discussed earlier, the ultimate conversion, α_C, (which was experimentally determined, cf. Figures 4 and 5) was observed to monotonically increase with increase in cure temperature.

From Figure 5, it is clear that the unmodified autocatalytic Kamal model [Eq. (9)], using the temperature dependent parameters listed in Table II, fit the experimental data well in the early stages of the cure. Deviations from autocatalytic cure kinetics may be observed in the later stages. On the other hand, the modified Kamal's model accounting for diffusion limited regime [eq. (13)] provides a good fit with the experimental curves for the entire conversion range, at all tested temperatures. The cure kinetics of this epoxy-anhydride system can therefore be described well using the modified Kamal autocatalytic kinetic equation incorporating a diffusion factor.

To facilitate convenient adaptation of this kinetic model for numerical simulations, average values of m and n have also been used to fit the experimental data. From the results in Table II, the average values for m and n are 0.38 and 1.19, respectively. Using these averaged values for m and n, k_1 and k_2 were recalculated by fitting the experimental data using eq. (9). The activation energies and the preexponential factors were then

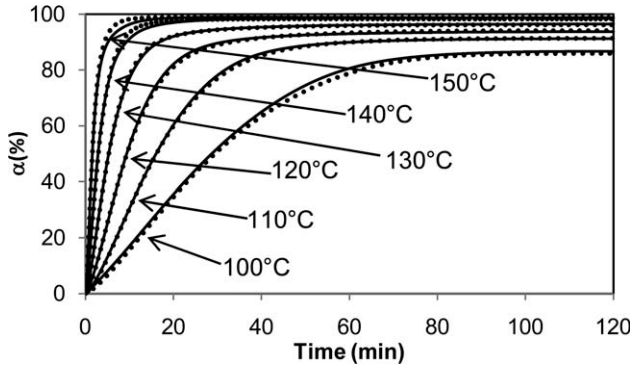

Figure 4. Conversion versus time at different temperatures (Solid curves indicate the experimental data and dotted curves indicate the fits obtained with the autocatalytic Kamal model modified to incorporate diffusion effects [eq. 13)], using the parameters listed in Table III).

Applied Polymer SCIENCE

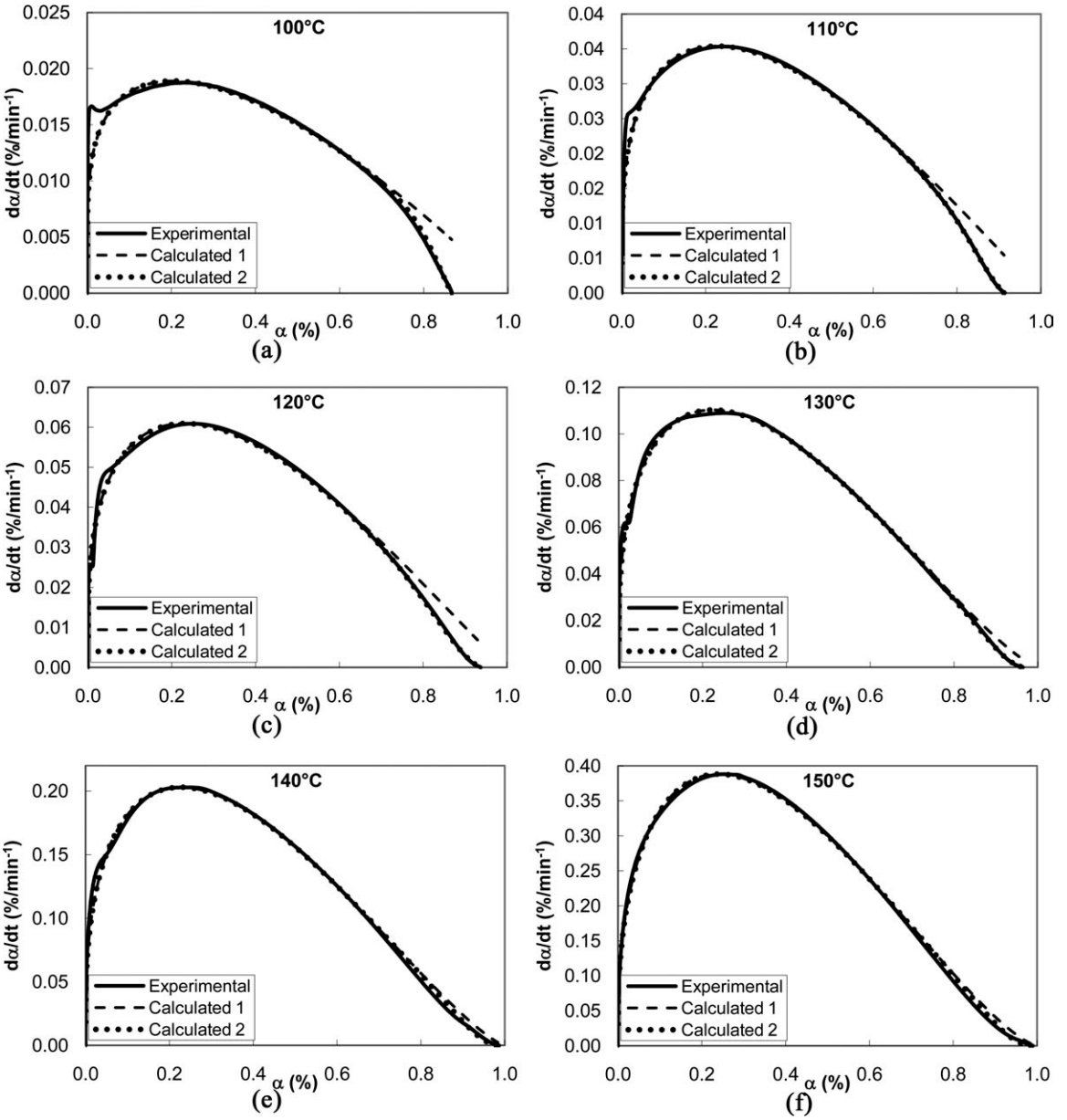

Figure 5. Rate of the cure reaction versus degree of cure at different temperatures. Experimental: Experimentally calculated reaction rates. Calculated 1: Reaction rates calculated using the Kamal's autocatalytic model [eq. (9)], with temperature dependent reaction orders *m* and *n*, and using kinetic model parameters listed in Table II; Calculated 2: Reaction rates calculated using the modified autocatalytic model [eq. (13)], with temperature dependent reaction orders *m* and *n*, and using kinetic model parameters listed in Table II.

Table II. Parameters for the Isothermal Model

Temperature (°C)	k_1 (min^{-1})		k_2 (min^{-1})		m	n	C	α_c
100	0.0033	ln A_1 = 13.32 ln(min^{-1}) $E_{\alpha 1}$ = 59.52 kJ/mol	0.0321	ln A_2 = 25.48 ln(min^{-1}) $E_{\alpha 2}$ = 89.78 kJ/mol	0.2886	0.9763	0.0375	0.8667
110	0.0039		0.0710		0.3428	1.0660	0.0477	0.9121
120	0.0078		0.1268		0.3694	1.1100	0.0599	0.9371
130	0.0119		0.2627		0.4113	1.3130	0.0425	0.9645
140	0.0161		0.4896		0.4067	1.3040	0.0403	0.9861
150	0.0312		1.0490		0.4674	1.3970	0.0420	0.9885
Average					0.3810	1.1944		

Table III. Parameters for the Isothermal Models with the Averaged *m* and *n*

Temperature (°C)	k_1 (min^{-1})		k_2 (min^{-1})		*m*	*n*	*C*	α_c
100	0.0033	$\ln A_1 = 13.33\ \ln(min^{-1})$ $E_{\alpha 1} = 59.52$ kJ/mol	0.0399	$\ln A_2 = 22.31\ \ln(min^{-1})$ $E_{\alpha 2} = 79.30$ kJ/mol	0.38	1.19	0.02149	0.8667
110	0.0039		0.0788				0.03346	0.9121
120	0.0078		0.1325				0.04494	0.9371
130	0.0119		0.2405				0.06386	0.9645
140	0.0161		0.4478				0.05904	0.9861
150	0.0312		0.8610				0.07697	0.9885

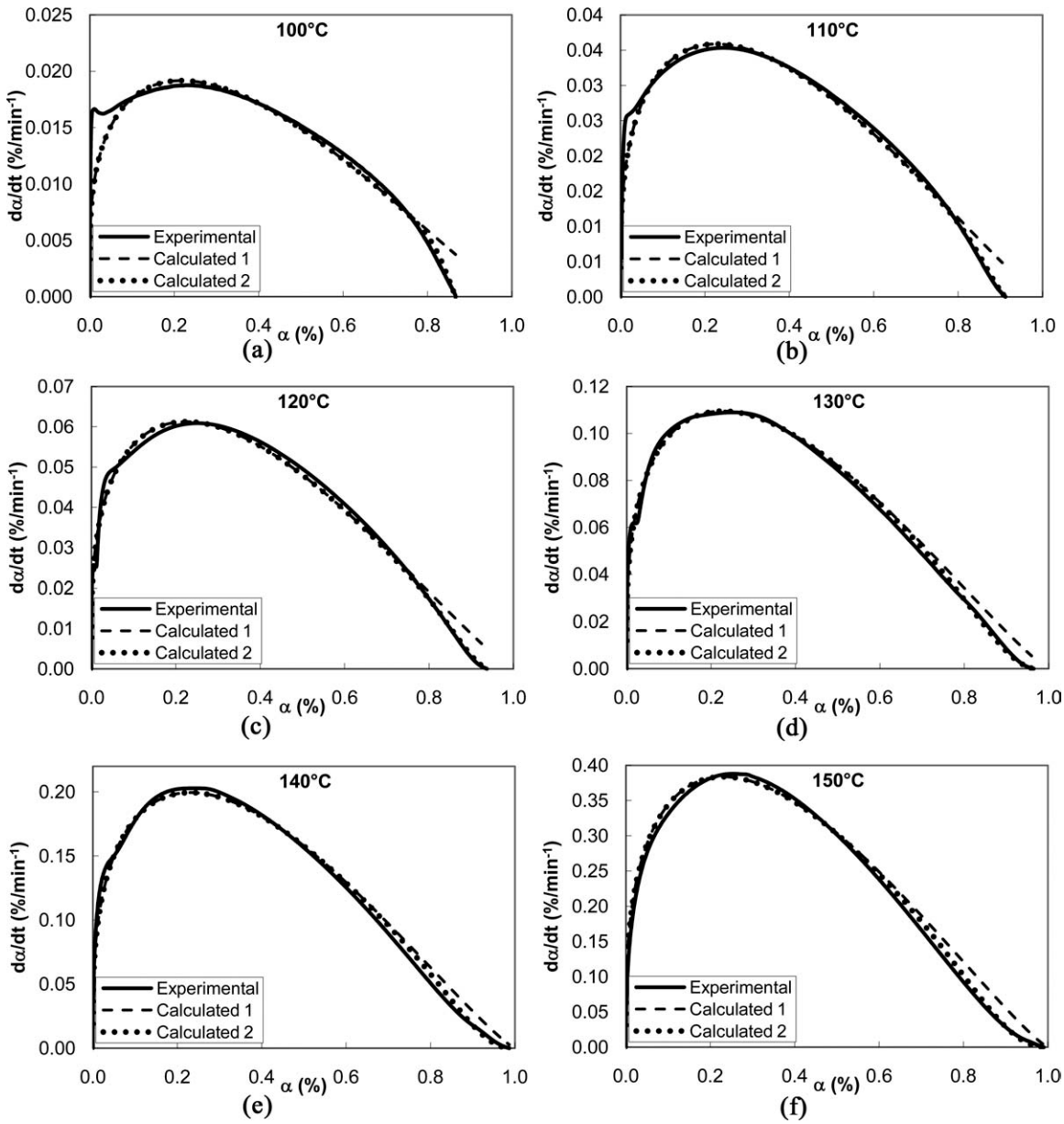

Figure 6. Rate of the cure reaction versus degree of cure at different temperatures. Experimental: Experimentally calculated reaction rates. Calculated 1: Reaction rates calculated using the Kamal's autocatalytic model [eq. (9)], with average reaction orders *m* and *n*, and using kinetic model parameters listed in Table III; Calculated 2: Reaction rates calculated using the modified autocatalytic model [eq. (13)], with average reaction orders m and n, and using kinetic model parameters listed in Table III.

calculated from k_1 and k_2 using eqs. (10) and (11). The results are summarized in Table III. E_{a1} and E_{a2} are calculated to be 59.52 and 79.30 kJ/mol, respectively. With these modified temperature-dependentk_1, and k_2, and averaged m and n from Table III, the parameter C in the diffusion factor was then calculated using eq. (13) for each temperature; these values are also listed in Table III. The values of experimentally observed α_C remain unchanged. The fits to experimental reaction rate versus conversion data, obtained with the purely autocatalytic Kamal model [eq. (9)] and the modified Kamal model with the diffusion factor incorporated [eq. (13)], using the averaged m and n, along with the parameters from Table III are displayed in Figure 6. From a comparison of the fits of the modified Kamal model with the diffusion factor in Figures 5 and 6, it can be noted that some degree of accuracy in fitting the experimental data is lost by averaging of m and n; however, the key experimental trends, such as the conversion corresponding to maximum reaction rate, are captured adequately. The diffusion-modified Kamal's model has also been verified through the curves of conversion versus time. Figure 4 displays the kinetic model fits. The calculated data using the parameters in Table III fit the experimental data well in the temperature range from 100 to 150°C.

CONCLUSIONS

The reaction kinetics of an anhydride cured epoxy thermoset resin system was characterized in nonisothermal as well as isothermal modes. Isothermal kinetics was studied at five different temperatures covering the range $T_g \pm 20$°C. Temperature-dependent ultimate conversion and reaction orders were indicative of strong diffusion effects. The simple Sestak–Berggren two parameter autocatlytic model was used to describe the nonisothermal cure behavior within the studied heating rates. Using Kamal's four parameter autocatalytic model, it was possible to describe isothermal kinetics of the reaction accurately in the early stages of the cure reaction in the temperature range were studied. However, to describe the kinetics in the later reaction stages satisfactorily, the model had to be modified to account for diffusion effects. Kamal's autocatalytic model was modified with a diffusion factor. In this manner, the resultant single kinetic model could describe the autocatalytic reaction as well as diffusion limited regimes, and also the temperature dependent ultimate conversion.

ACKNOWLEDGMENTS

The authors would like to thank Drs. Libby Berger, Hamid Kia, Stefan Slavik, John Owens, and Arun M. Kumar for helpful discussions.

REFERENCES

1. Wisnom, M. R.; Gigliotti, M.; Ersoy, N.; Campbell, M.; Potter, K. D. *Compos. A: Appl. Sci.* **2006,** *37*, 522.
2. Pillai, V.; Beris, A. N.; Dhurjati, P. *J. Compos. Mater.* **1997,** *31*, 22.
3. Capehart, T. W.; Muhammad, N.; Kia, H. G. *J. Compos. Mater.* **2007,** *41*, 1675.
4. Bogetti, T. A.; Gillespie J. W., Jr. *J. Compos. Mater.* **1992,** *26*, 626.
5. Zhao, L. G.; Warrior, N. A.; Long, A. C. *Int. J. Solids. Struct.* **2006,** *43*, 5449.
6. Ernst, L. J.; Jansen, K. M. B.; Saraswat, M.; vant Hof, C.; Zhang, G. Q.; Yang, D. G.; Bressers, H. J. L. IEEE 2006 7th International Conference on Electronics Packaging Technology, Shanghai, China, August 26–30, **2006**
7. Prasatya, P.; McKenna, G. B.; Simon, S. L. *J. Compos. Mater.* **2001,** *35*, 826.
8. Montserrat, S. J.; Male, J. *Thermochim. Acta.* **1993,** *228*, 47.
9. Malek, J. *Thermochim. Acta.* **2000,** *355*, 239.
10. Malek, J. *Thermochim. Acta.* **1992,** *200*, 257.
11. Sestak, J.; Berggren, G. *Thermochim. Acta.* **1971,** *3*, 1.
12. Acitelli, M. A.; Prime, R. B.; Sacher, E. *Polymer.* **1971,** *12*, 35.
13. Ryan, M. E. *Polym. Eng. Sci.* **1984,** *24*, 698.
14. Kamal, M. R.; Ryan, M. E. *Polym. Eng. Sci.* **1980,** *20*, 859.
15. Han, C. D.; Lem, K. W. *Polym. Eng. Sci.* **1984,** *24*, 473.
16. Kamal, M. R. *Polym. Eng. Sci.* **1974,** *14*, 230.
17. Sourour, S.; Kamal, M. R. *Thermochim. Acta.* **1976,** *14*, 41.
18. Yousefi, A.; Lafleur, P. G.; Gauvin, R. *Polym. Compos.* **1997,** *18*, 157.
19. Ng, H.; Manas-Zloczower, I. *Polym. Eng. Sci.* **1989,** *29*, 302.
20. Kissinger, H. E. *Anal. Chem.* **1957,** *29*, 1702.
21. Coats, A. W.; Redfern, J. P. *Nature* **1964,** *68*, 201.
22. Rosu, D.; Cascaval, C. N.; Mustata, F.; Ciobanu, C. *Thermochim. Acta.* **2002,** *383*, 119.
23. Fournier, J.; Williams, G.; Duch, C.; Addridge, G. A. *Macromolecules* **1996,** *29*, 7097.
24. Cole, K. C.; Hechler, J. J.; Noel, D. *Macromolecules* **1991,** *24*, 3098.
25. Xie, H.; Liu, B.; Sun, Q.; Yuan, Z.; Shen, J.; Cheng, R. *J. Appl. Polym. Sci.* **2005,** *96*, 329.
26. Jenninger, W.; Schawe, J. E. K.; Alig, I. *Polymer* **2000,** *41*, 1577.